DAPT-Induced Intracellular Accumulations of Longer Amyloid β-Proteins: Further Implications for the Mechanism of Intramembrane Cleavage by γ-Secretase†

Sousuke Yagishita,‡,§ Maho Morishima-Kawashima,*,‡ Yu Tanimura,‡ Shoichi Ishiura,§ and Yasuo Ihara*,‡

Department of Neuropathology, Faculty of Medicine, University of Tokyo, Tokyo 113-0033, Japan, and Department of Life Science, Graduate School of Arts and Science, University of Tokyo, Tokyo 153-8902, Japan

Received October 25, 2005; Revised Manuscript Received December 2, 2005

ABSTRACT: γ-Secretase cleaves the transmembrane domain of β-amyloid precursor protein at multiple sites. These are referred to as γ-, ζ-, and ϵ-cleavages. We showed previously that DAPT, a potent dipeptide γ-secretase inhibitor, caused differential accumulations of longer amyloid β-proteins (Aβs) (Aβ43 and Aβ46) in CHO cells that are induced to express the β C-terminal fragment (CTF). To learn more about the cleavage mechanism by γ-secretase, CHO cell lines coexpressing βCTF and wild-type or mutant presenilin (PS) 1/2 were generated and treated with DAPT. In all cell lines treated with DAPT, as the levels of Aβ40 decreased, Aβ46 accumulated to varying extents. In wild-type PS1 or M146L mutant PS1 cells, substantial amounts of Aβ43 and Aβ46 accumulated. In contrast, this was not the case with wild-type PS2 cells. In M233T mutant PS1 cells, significant amounts of Aβ46 and Aβ48 accumulated differentially, whereas in N141I mutant PS2 cells, large amounts of Aβ45 accumulated concomitantly with a large decrease in Aβ42 levels. Most interestingly, in G384A mutant PS1 cells, there were no significant accumulations of longer Aβs except for Aβ46. Aβ40 was very susceptible to DAPT, but other Aβs were variably resistant. Complicated suppression and accumulation patterns by DAPT may be explained by stepwise processing of βCTF from a ζ- or ϵ-cleavage site to a γ-cleavage site and its preferential suppression of γ-cleavage over ζ- or ϵ-cleavage.

Senile plaques, one of the neuropathological hallmarks of Alzheimer's disease (AD),[1] are composed of a small ~40-residue protein called amyloid β-protein (Aβ). Aβ is produced from β-amyloid precursor protein (APP), through sequential cleavages by two membrane proteases referred to as β- and γ-secretases (*1*). β-Secretase or β-site APP-cleaving enzyme (BACE) (*2*) is a membrane-bound aspartyl protease and cleaves APP in its luminal portion, generating a 99-residue fragment called β C-terminal fragment (CTF). βCTF in turn is cleaved by γ-secretase in the middle of its transmembrane domain. Thus, generated Aβ is finally secreted into the extracellular space. While the most predominant product is Aβ40, a two-residue longer species, Aβ42, was found to predominate in senile plaques and is believed to be the species initially deposited in the brain (*3*). It was recently demonstrated that the mice that exclusively produce Aβ42 develop amyloid deposition in the brain parenchyma, whereas those producing Aβ40 do not (*4*). This is probably because Aβ42 has a much higher aggregation potential than Aβ40. Thus far, three causative genes for familial AD (FAD), *APP*, *presenilin (PS) 1*, and *PS2*, have been identified. In accordance with the above, the FAD mutations lead to an increased production of Aβ42, indicating a pivotal role of Aβ42 for the development of AD (*1*).

The mechanism of intramembrane cleavages at the Aβ40 and Aβ42 sites by γ-secretase has remained completely an enigma. Accumulating evidence suggests that γ-secretase is also an aspartyl protease with its catalytic site(s) sitting within the membrane (*5*). The substitution of one or two highly conserved Asp residues in the transmembrane domains 6 and 7 of PS1 and PS2 led to a profound loss of the γ-secretase activity (*6*, *7*). Thus, PS1/2 appear to compose the catalytic core of γ-secretase. Whereas signal peptide peptidase, another member of the PS family, functions by itself (*8*), γ-secretase is composed of multiple membrane proteins (*9*). Active γ-secretase is assumed to take the form of a high-molecular-weight multiprotein complex consisting of at least four integral membrane proteins, PS, Aph-1, nicastrin, and Pen-2, all of which are essential for full γ-secretase activity (*10*−*12*).

γ-Secretase cleaves APP (βCTF) in the middle of the transmembrane domain (γ-cleavage), releasing Aβ, and near the membrane−cytoplasm boundary (ϵ-cleavage), producing APP intracellular domain (AICD) (*13*−*16*). ϵ-Cleavage generates AICD50−99, a major product, and AICD49−99, a minor product (*13*). Although the relationship between γ-

† This work was supported in part by a grant-in-aid for Scientific Research on Priority Areas, Advanced Brain Science Project, from the Ministry of Education, Culture, Sports, Science, and Technology, Japan.

* To whom correspondence should be addressed: Department of Neuropathology, Faculty of Medicine, University of Tokyo, 7-3-1 Hongo, Bunkyo-ku, Tokyo 113-0033, Japan. Telephone: +81-3-5841-3541. Fax: +81-3-5800-6854. E-mail: yihara@m.u-tokyo.ac.jp (Y.I.); maho@m.u-tokyo.ac.jp (M.M.-K.).

‡ Department of Neuropathology, Faculty of Medicine, University of Tokyo.

§ Department of Life Science, Graduate School of Arts and Science, University of Tokyo.

[1] Abbreviations: AD, Alzheimer's disease; Aβ, amyloid β-protein; APP, β-amyloid precursor protein; BACE, β-site APP-cleaving enzyme; CTF, C-terminal fragment; FAD, familial Alzheimer's disease; PS, presenilin; AICD, APP intracellular domain; wt, wild type; mt, mutant; CHO, Chinese hamster ovary.

10.1021/bi0521846 CCC: $33.50
Published on Web 03/01/2006

and ϵ-cleavages is still not well-understood, our previous study showed some correlations between the major counterparts, Aβ40 versus AICD50−99, and between the minor counterparts, Aβ42 versus AICD49−99 (*17*). We further showed that truncated βCTFs that terminate in the ϵ-sites (Aβ49 and Aβ48) can be processed to Aβ40/42 in a γ-secretase-dependent manner (*18*, see also ref *19*). Those ϵ-cleavage sites affect the production of Aβ40/42: Aβ49 predominantly produces Aβ40, while Aβ48 preferentially produces Aβ42. This indicates that there is some link between γ- and ϵ-cleavages. Recently, ζ-cleavage, that occurs between γ- and ϵ-cleavage sites and generates Aβ46, has been identified (*20*). We independently identified several longer Aβs within cells and in the brain, including Aβ43, Aβ45, Aβ46, and Aβ48 (*21*). Moreover, the treatment with DAPT, a potent dipeptide γ-secretase inhibitor, was found to induce the accumulation of Aβ43 and subsequently Aβ46, following a large decrease in the Aβ40 levels, in the Chinese hamster ovary (CHO) cells (*21*). Thus, it is likely that βCTF undergoes γ-secretase-mediated cleavages at multiple sites within its transmemebrane domain. These cleavage sites are aligned on the α-helical surface of the transmembrane domain, and we speculated that βCTF is processed at every third residue by γ-secretase (*21*). To further test this hypothesis, we investigate here whether DAPT induces similar effects on the intracellular levels of longer Aβs in wild-type (wt) or mutant (mt) PS1- and PS2-transfected cells.

EXPERIMENTAL PROCEDURES

Cell Culture. CHO cells expressing βCTF (C99 cells) inducibly in the presence of 1 μg/mL tetracycline (Invitrogen, Carlsbad, CA) (*21*) were maintained in a F-12 nutrient mixture (Invitrogen) containing 10% fetal bovine serum (Invitrogen), penicillin/streptomycin, 250 μg/mL Zeocin (Invitrogen), and 10 μg/mL Blasticidine S (Invitrogen). Other stably transfected cell lines generated for the present study were cultured in the above medium supplemented with 200 μg/mL G418 (Calbiochem, San Diego, CA).

Generation of Cell Lines. A mammalian expression vector pcDNA3.1 (Invitrogen) containing human wtPS1, G384A or M233T mtPS1, wtPS2, or N141I mtPS2 cDNA was transfected to C99 cells using Lipofectamine 2000 (Invitrogen) according to the instructions of the manufacturer, and the stable cell lines (C99/wt or mtPS1/2 cells) were selected with 500 μg/mL G418. The plasmid containing M146L mtPS1 was generated by the polymerase chain reaction using the plasmid containing wtPS1 and oligonucleotide primers, 5′-GTC ATT GTT GTC CTC ACT ATC CTC CTG-3′ and 5′-CAG GAG GAT AGT GAG GAC AAC AAT GAC-3′. M146L mtPS1 cDNA was subcloned into pIRESneo3, a mammalian expression vector (BD Biosciences, Palo Alto, CA). The obtained plasmid was transfected to C99 cells using Lipofectamine 2000, and the stable cell lines (C99/M146L mtPS1 cells) were selected with 500 μg/mL G418.

Antibodies. Monoclonal antibodies against Aβ used in this study were 6E10 (raised against Aβ1−17) (Signet Laboratories, Dedham, MA), BAN50 (raised against Aβ1−16) (*22*), and 82E1 (an N-end-specific antibody against Asp-1 of human Aβ) (IBL, Fujioka, Japan) (*21*). A polyclonal antibody used for the detection of βCTF and AICD was C4 (raised against the 30-residue cytoplasmic domain of APP). PS1/2 antibodies used were as described elsewhere (*23*).

Treatment with γ-Secretase Inhibitors. γ-Secretase inhibitors used here were {1*S*-benzyl-4*R*-[1*S*-carbamoyl-2-phenylethylcarbamoyl-1*S*-3-methylbutylcarbamoyl]-2*R*-hydroxy-5-phenylpentyl} carbamic acid *tert*-butyl ester (L685,458) (*24*), *N*-[*N*-(3,5-difluorophenacetyl)-L-alanyl]-*S*-phenylglycine *tert*-butyl ester (DAPT) (*25*), *N*-[*N*-(3,5-difluorophenacetyl)]-L-alanyl]-3-(*S*)-amino-1-methyl-5-phenyl-1,3-dihydrobenzo[*e*](1,4)diazepin-2-one (compound E) (*26*), 1-(S)-endo-*N*-(1,3,3-trimethylbicyclo[2.2.1]hept-2-yl)4-fluorophenyl sulfonamide (sulfonamide) (*27*), and WPE-III-31C (*28*). All of the inhibitors were purchased from Calbiochem.

Cells were incubated with each γ-secretase inhibitor at indicated concentrations for 2 h and then cultured in the presence of 1 μg/mL tetracycline and each γ-secretase inhibitor for 4 h.

Preparation of Cell Lysates and Immunoprecipitation of Aβ. After harvested cells were thoroughly washed with phosphate-buffered saline, they were suspended in 2% SDS and 50 mM Tris-HCl at pH 7.6 with brief sonication. Equal protein amounts of the cell lysates were subjected to Western blotting using Tris/Tricine conventional gels to assess the levels of total Aβ.

Harvested cells were homogenized with four volumes of Tris-buffered saline (50 mM Tris-HCl at pH 7.6, 150 mM NaCl, and 1 mM EGTA) containing 1% Triton X-100 and various protease inhibitors (0.1 mM diisopropyl fluorophosphate, 0.1 mM phenylmethylsulfonyl fluoride, 5 μg/mL N^{α}-*p*-tosyl-L-lysine chloromethyl ketone, 1 μg/mL antipain, 1 μg/mL pepstatin, 1 μg/mL leupeptin, 1 μg/mL bestain, 1 μg/mL amerstain, 5 mM 1,10-phenanthroline monohydrate, and 1 mM thiorphan). The homogenates were spun at 540000*g* for 20 min. Each supernatant was appropriately diluted to the same protein concentrations, and an equal volume of the lysate was subjected to immunoprecipitation. The cell lysates were first incubated with C4-bound protein A-Sepharose at 4 °C for 2 h to remove βCTF, and the resultant supernatants were immunoprecipitated further with BAN50 at 4 °C for 6 h. The immune complexes were collected with protein G-Sepharose and eluted with the SDS sample buffer. The immunoprecipitated proteins were separated on Tris/Tricine/8 M urea gels, followed by Western blotting.

Tris/Tricine/8 M Urea Gels and Western Blotting. To assess the levels of total Aβ, a conventional 16.5% acrylamide Tris/Tricine gel was run and the blot was probed with 6E10 or 82E1. Various longer Aβ species were separated on a Tris/Tricine/8 M urea gel with minor modifications (*21*). A 11% T/3% C separation gel at pH 8.45 containing 8 M urea and 2.8% glycerol (gel system I) was used to separate Aβ37−45. A 12% T/3% C separation gel at pH 8.90 containing 8 M urea and 2.0% glycerol (gel system II) was used to separate Aβ46−49. Each separation gel (length of 16 cm) was overlayed with a 10% T/3% C spacer gel (0.5 cm; pH 8.45) and a 4% T/3% C stacking gel (0.5 cm; pH 8.45) that did not contain urea. The cathode buffer [0.1 M Tris, 0.1 M Tricine, 0.1% (w/v) SDS] was the same for both systems. The anode buffer was 0.2 M Tris/HCl at pH 8.90 and 25 °C for gel system I and was 0.2 M Tris/HCl at pH 9.00 and 25 °C for gel system II. After transfer, the blots were probed with 82E1 to detect only Aβs that begin at Asp-1 and developed using an ECL system. Intensities of the bands were quantified using a LAS-1000plus luminescent image analyzer (Fuji Film, Tokyo, Japan).

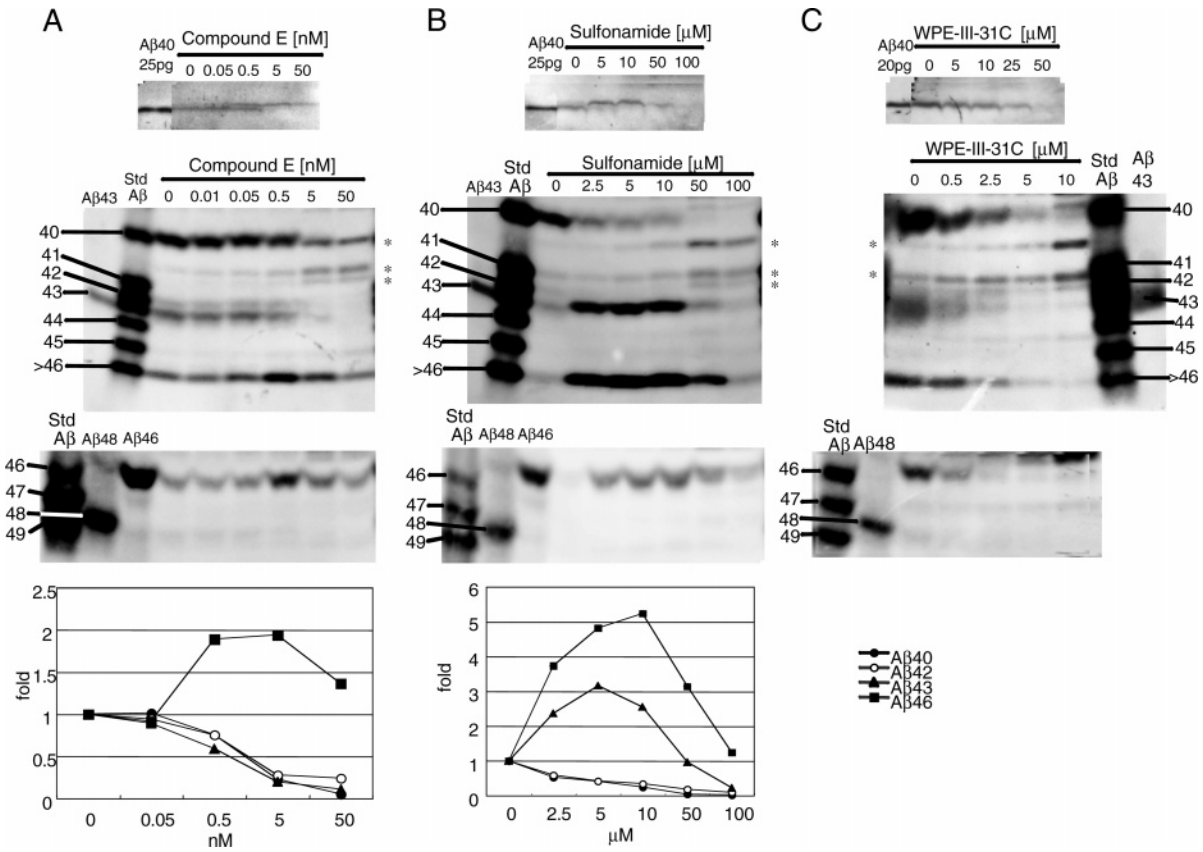

FIGURE 1: Effects of various γ-secretase inhibitors on the levels of longer Aβs. C99 cells were treated with either compound E (A), sulfonamide (B), or WPE-III-31C (C) at the indicated concentrations for 2 h, and βCTF was induced for 4 h with tetracycline in the presence of each inhibitor. Equal amounts of protein from the cell lysates were subjected to conventional Tris/Tricine gel electrophoresis, followed by Western blotting with 6E10 to assess the total intracellular Aβ (top panels). Synthetic Aβ40 (20 or 25 pg) was loaded in the leftmost lane. Triton X-100-soluble fractions from the treated cells were immunoprecipitated with BAN50, and collected Aβs were separated by gel system I (second panels) or gel system II (third panels), followed by Western blotting with 82E1. Synthetic Aβs (30−50 pg for each species) were loaded in the left two or three lanes of each panel, as marked. The representative Western blots are shown here. The bands indicated by an asterisk are presumably C-terminally truncated βCTFs, which exhibit varying mobilities relative to those of synthetic Aβs under different gel conditions. The levels of intracellular Aβ were quantified using LAS-1000plus luminescent image analyzer (bottom panels in A and B), with the levels of each Aβ species in the nontreated cells being assumed 1. The plots represent the means of the values from three (A) or four (B) independent experiments. Compound E induced an accumulation of Aβ46 (A), and sulfonamide induced accumulations of Aβ43 and Aβ46 (B), whereas WPE-III-31C suppressed the levels of Aβs uniformly (C).

Other Methods. Protein concentrations were determined using the bicinchoninic acid protein assay reagent (Pierce, Rockford, IL). All longer Aβ proteins, from Aβ1−44 to Aβ1−49, were synthesized using an automated peptide synthesizer (ABI 433A, Applied Biosystems, Foster City, CA). Crude Aβ proteins were partially purified by size-exclusion chromatography on Superdex 75 10/300 GL (10 × 300 mm) and Superdex peptide 10/300 GL (10 × 300 mm) (Amersham Biosciences Corp., Piscataway, NJ) columns and were eluted with 20% 2-propanol/80% formic acid (v/v) at a flow rate of 0.4 mL/min (*21*).

RESULTS

Accumulations of Longer Aβs with Nontransition-State γ-Secretase Inhibitors other than DAPT. Our previous study showed that treatment with DAPT caused intracellular accumulations of longer Aβs in C99 cells that can be induced to express βCTF, an immediate substrate for γ-sectetase (*21*). Concomitant with a large decrease in the levels of Aβ40, there was an accumulation of Aβ43, followed by Aβ46. Thus, we first sought to see if other γ-secretase inhibitors induce similar differential accumulations of intracellular longer Aβs.

Compound E and sulfonamide, two other nontransition-state inhibitors, produced similar but not identical effects in C99 cells (Figure 1). In contrast to DAPT, compound E reduced the levels of Aβ43 as well as Aβ40 and Aβ42 (Figure 1A). These gradual decreases were accompanied by a gradual increase and subsequent decrease in the levels of Aβ46. The treatment with sulfonamide gave a similar decay profile for Aβ40 and Aβ42 (Figure 1B). After these decreases, the levels of Aβ43 and Aβ46 increased and subsequently decreased in a similar manner, although the former reached a maximum at the lower sulfonamide concentration. The levels of total intracellular Aβ decreased, and the mobility of Aβ on conventional Tris/Tricine gels became slower, as the concentrations of compound E and sulfonamide increased (parts A and B of Figure 1). This mobility shift should reflect the accumulation of longer Aβs (see below). In a sharp contrast, WPE-III-31C, a transition-state analogue γ-secretase inhibitor, suppressed uniformly the levels of all of the Aβ species (Figure 1C), a characteristic that was also shared by L685,458 (*21*).

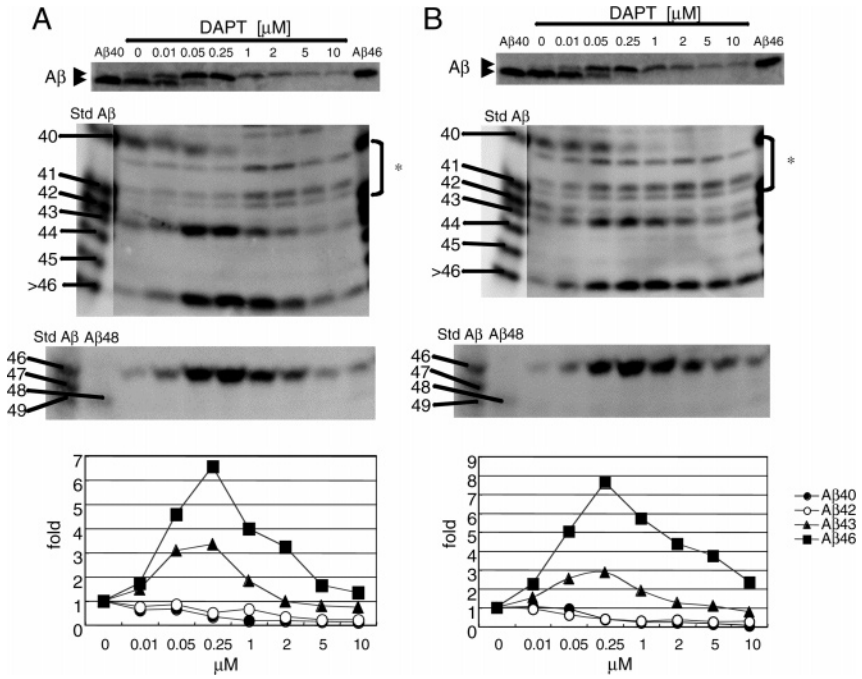

FIGURE 2: Dose-dependent effects of DAPT on the levels of longer Aβs in C99/wtPS1 cells (A) and C99/M146L mtPS1 cells (B). The cells were cultured with indicated DAPT concentrations for 2 h and then with 1 μg/mL tetracycline and DAPT for 4 h to induce βCTF. Equal amounts of protein from the cell lysates were subjected to conventional Tris/Tricine gel electrophoresis, followed by Western blotting with 82E1 to assess the total levels of intracellular Aβ (top panels). Synthetic Aβ40 and Aβ46 (8 pg for each) were loaded in the leftmost and rightmost lanes, respectively. The total intracellular Aβs were resolved into two components, slow Aβ and fast Aβ (arrowheads). Aβs in the cell lysates were immunoprecipitated with BAN50, separated on gel system I (second panels) or gel system II (third panels), and subjected to Western blotting with 82E1. It should be noted that Aβ species have probably varying retaining efficiencies on the blots, and the amount of a certain Aβ species cannot be compared with that of another Aβ species with a different mobility. Synthetic Aβs (30−50 pg for each species) were loaded into one or two leftmost lanes, as marked. The representative Western blots are shown here. The bands indicated by an asterisk are presumably C-terminally truncated βCTFs. The levels of intracellular Aβ were quantified using LAS-1000plus luminescent image analyzer (bottom panels), with the levels of each Aβ species in the nontreated cells being assumed 1. The plots represent the means of the values from three (Aβ40, Aβ43, and Aβ46 in A and B and Aβ42 in B) or two (Aβ42 in A) independent experiments. In both cell lines, Aβ43 and Aβ46 accumulated concomitantly with a gradual decrease in Aβ40 levels.

DAPT-Induced Accumulations of Aβ43 and Aβ46 in C99/wtPS1 Cells and C99/M146L mtPS1 Cells. To further investigate the relationship between DAPT treatment and accumulations of longer Aβs, we examined whether DAPT led to intracellular accumulations of longer Aβs in PS1/2-transfected cells in a manner similar to parental C99 cells and which kind of longer Aβs accumulates in mtPS1/2 cells that produce higher proportions of Aβ42.

For this purpose, we generated six stable cell lines by transfecting wt or various mtPS1/2 cDNA to C99 cells and the established cell lines (C99/wt or mtPS1/2 cells) were treated with DAPT. In these stable cell lines, the endogenous hamster PS1 fragments were almost completely displaced with newly introduced human wt or mtPS1/2 (see Figure S1 in the Supporting Information) and βCTF induced by tetracycline was found at almost the same level across the cell lines (data not shown). The proportions of intracellular Aβ42 were increased significantly in C99/M146L mtPS1 cells or remarkably in C99/M233T and C99/G384A mtPS1 cells and C99/N141I mtPS2 cells, as compared with those in C99/wtPS1/2 cells (data not shown), an observation that is consistent with the previous study in the CHO cells that stably coexpress full-length APP and wt or mtPS1/2 (*23*).

Careful inspection revealed that intracellular Aβ in C99/wtPS1 or C99/M146L cells consisted of two closely spaced bands on conventional Tris/Tricine gels. The levels of Aβ with fast mobility (fast Aβ) decreased up to 0.05 μM DAPT, while those of Aβ with slow mobility (slow Aβ) increased up to 0.25 μM and then decreased (Figure 2). As expected, the levels of Aβ42 were substantially higher in C99/M146L cells than in C99/wtPS1 cells. In both cell lines, the levels of Aβ40 and Aβ42 decreased as DAPT concentrations increased. After these decreases, those of Aβ43 and Aβ46 gradually increased, peaked at 0.25 μM, and then declined. It should be noted that Aβ49, a counterpart of AICD50−99, was consistently undetectable, which confirmed the previous observation (*21*). Accumulation of Aβ46 continued more than that of Aβ43 up to higher DAPT concentrations, and the former levels decreased only gradually. Thus, it is likely that fast Aβ separated on Tris/Tricine gels consists mainly of Aβ40 and Aβ42, while slow Aβ consists of Aβ46. In fact, these two closely separated bands exactly corresponded with those of synthetic Aβ40/42 and Aβ46 when coelectrophoresed (upper panel of Figure 2). Thus, these two PS1 cell lines exhibited differential accumulations of longer Aβs in response to DAPT, although sequential accumulations of Aβ43 and Aβ46 were somewhat indistinct. In a sharp contrast, L685,458 uniformly suppressed the levels of all of the Aβs (data not shown).

Secreted Aβ species in the medium of C99/wtPS1 cells were similarly examined. Substantial amounts of Aβ40 and Aβ42 and a very small amount of Aβ43 but not even a trace amount of Aβ46 were detectable in the medium in the absence of DAPT (data not shown). The amounts of secreted

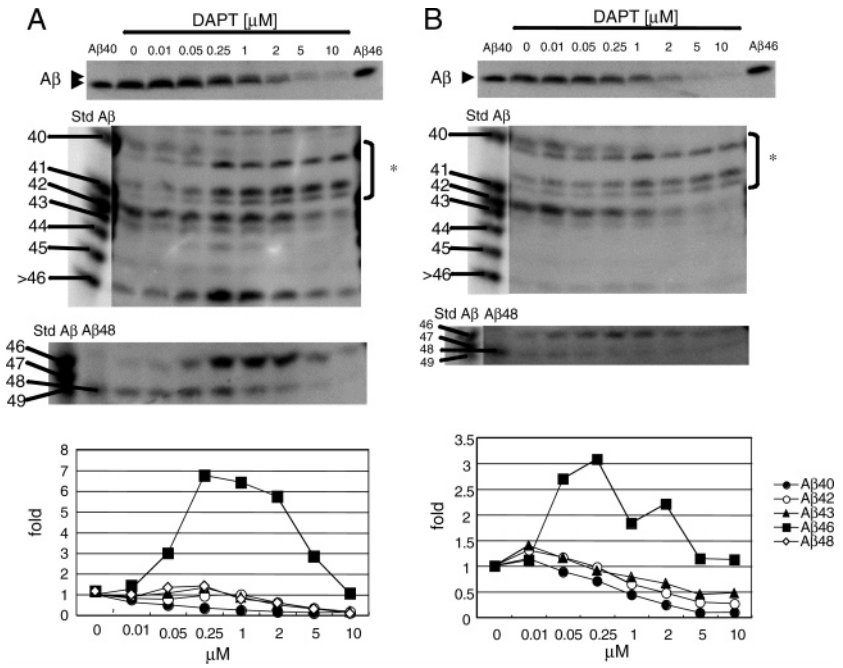

FIGURE 3: Dose-dependent effects of DAPT on the levels of longer Aβs in C99/M233T mtPS1 cells (A) and C99/G384A mtPS1 cells (B). Equal amounts of protein from the cell lysates were subjected to conventional Tris/Tricine gel electrophoresis, followed by Western blotting with 82E1 to assess the levels of total intracellular Aβ (top panels). Synthetic Aβ40 and Aβ46 (8 pg for each) were loaded in the leftmost and rightmost lanes, respectively. Total Aβ was resolved into two components in C99/M233T mtPS1 cells (A) but not in C99/G384A mtPS1 cells (B). BAN50 immunoprecipitates were separated by gel system I (second panels) or gel system II (third panels), followed by Western blotting with 82E1. Synthetic Aβs (30−50 pg for each species) were loaded in one or two leftmost lanes, as marked. The representative Western blots are shown here. The bands indicated by an asterisk are presumably C-terminally truncated βCTFs. The levels of intracellular Aβ were quantified using LAS-1000plus luminescent image analyzer (bottom panels), with the levels of each Aβ in the nontreated cells being assumed 1. The plots represent the means of the values from three (Aβ40, Aβ42, Aβ43, and Aβ48 in A) or two (Aβ46 in A and all species in B) independent experiments. Aβ46 and Aβ48 accumulated differentially in C99/M233T cells (A), whereas longer Aβs did not accumulate in C99/G384A cells, except for Aβ46 that showed a low extent of accumulation (B).

Aβ43 did not increase, and Aβ46 was not detected in the medium even by the treatment with DAPT. This was the case with other cell lines studied here.

Significant Accumulations of Aβ46 and Aβ48 in C99/M233T mtPS1 Cells versus Slight Accumulation of Aβ*46 in C99/G384A mtPS1 Cells.* We then investigated the effects of DAPT on the mtPS1 cell lines, C99/M233T and C99/G384A, both of which produced much larger proportions of Aβ42 than did C99/wtPS1 cells. With increasing DAPT concentrations, the levels of total Aβ gradually decreased in both cell lines (parts A and B of Figure 3). At more than 5 μM, total Aβ was almost undetectable. In C99/M233T cells, Aβ was resolved into two components on Tris/Tricine gels, a similar alteration as found in C99/M146L cells (Figure 3A). In contrast, the total Aβ from C99/G384A mtPS1 cells no longer split on the gel (Figure 3B).

In C99/M233T cells, Tris/Tricine/8 M urea gel electrophoresis showed that Aβ40 declined gradually and became indiscernible at 1 μM DAPT (Figure 3A). The levels of Aβ42 were sustained up to 1 μM and declined subsequently at concentrations greater than 2 μM. Thus, the levels of Aβ42 were less susceptible to DAPT than those of Aβ40. The accumulation of Aβ43 was barely apparent, and its levels decreased in parallel with Aβ42. On the other hand, the levels of Aβ46 increased at 0.05 μM, reached a maximum at 0.25 μM, and declined at concentrations greater than 0.25 μM. Aβ48 was obviously detectable even before the DAPT treatment, and its level increased to a very small peak at 0.25 μM and then declined.

In C99/G384A cells, the levels of Aβ40 and Aβ42 decreased gradually (Figure 3B), with the latter decreasing more gradually. Aβ40 was hardly detectable at 1 μM DAPT, while Aβ42 was detectable even at 2 μM. Aβ43 and Aβ48 were barely discernible and seemed to decline gradually. There was minimal accumulation of Aβ46 (second panel of Figure 3B). This is consistent with the findings of Tris/Tricine gels that there is no apparent generation of slow Aβ (top panel of Figure 3B). The treatment with L685,458 suppressed the levels of all of the Aβ species in a similar dose-dependent manner (data not shown).

A Minimal Accumulation of Aβ46 in C99/wtPS2 Cells and a Marked Accumulation of Aβ45 in C99/N141I Cells. We next investigated whether the accumulation of longer Aβs was similarly induced by DAPT in C99 cells harboring PS2 instead of PS1. Total Aβ in C99/wtPS2 cells decreased steeply with increasing concentrations of DAPT and became indiscernible at 0.25 μM (Figure 4A), which contrasts with C99/wtPS1 cells in which the total Aβ was discernible even at 10 μM (Figure 2A). Tris/Tricine/8 M urea gels showed that the levels of Aβ40 and Aβ42 decreased rather abruptly, and both were barely discernible at 0.25 μM. Whereas Aβ43 did not accumulate, the very low levels of Aβ46 increased gradually to a maximum at 0.25−1 μM and then declined. It should be noted that the extent of Aβ46 accumulation was much smaller than those in C99/wtPS1 cells. Interestingly, two faint bands comigrating with synthetic Aβ48 and Aβ49 were reproducibly detected (Figure 4A). The intensities of

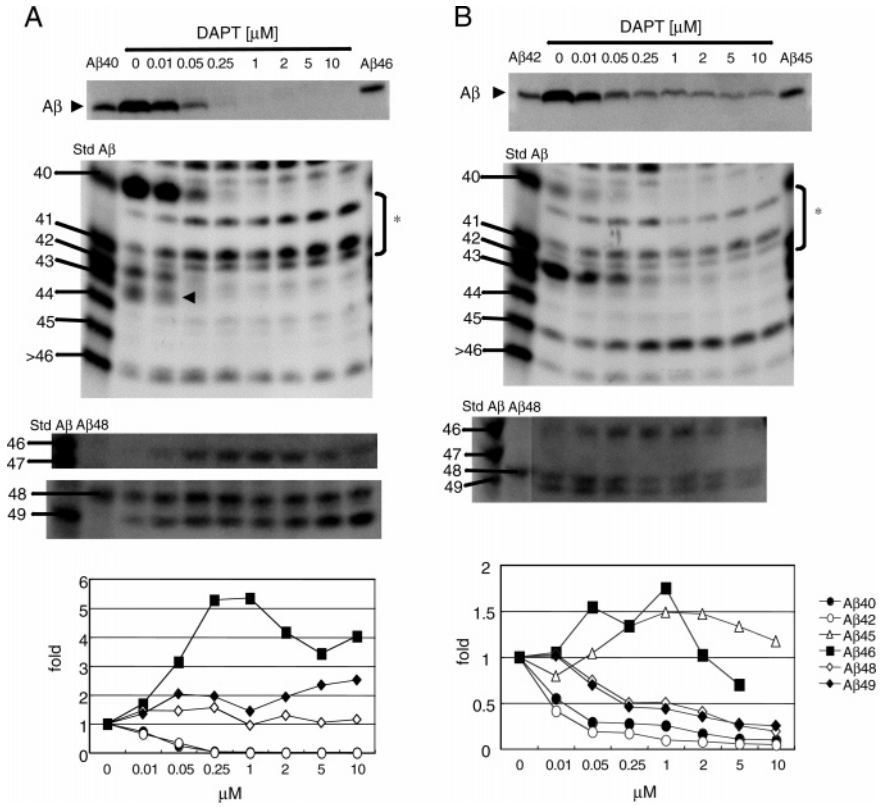

FIGURE 4: Dose-dependent effects of DAPT on the levels of longer Aβs in C99/wtPS2 cells (A) and C99/N141I mtPS2 cells (B). Equal amounts of protein from the cell lysates were subjected to conventional Tris/Tricine gel electrophoresis, followed by Western blotting with 82E1 to assess the levels of total intracellular Aβ (top panels). The leftmost and rightmost lanes in A and B are synthetic Aβ40 and Aβ46, and Aβ42 and Aβ45 (8 pg for each), respectively. The levels of total Aβ decreased steeply in C99/wtPS2 cells (A). In C99/N141I cells, the total Aβ levels decreased, accompanying a slight mobility shift on Tris/Tricine SDS gels (B). BAN50 immunoprecipitates were separated by gel system I (second panels) or gel system II (third panels), followed by Western blotting with 82E1. In C99/wtPS2 cells, only Aβ46 accumulated to low levels. An arrowhead represents what is presumed to be an Aβ shorter than Aβ37 (A). The representative Western blots are shown here. The bands indicated by an asterisk are presumably C-terminally truncated βCTFs. The levels of intracellular Aβ were quantified using LAS-1000plus luminescent image analyzer (bottom panels), with the levels of each Aβ species in the nontreated cells being assumed 1. The plots represent the means of the values from three (Aβ40, Aβ42, and Aβ46 in A and Aβ40, Aβ42, Aβ45, Aβ48, and Aβ49 in B) or two (Aβ48 and Aβ49 in A and Aβ46 in B) independent experiments. In C99/N141I cells, Aβ45 accumulated remarkably, following a steep decrease in the levels of Aβ42 (second panel in B).

the latter slightly increased with increasing DAPT concentrations, and the presumed Aβ49 did not significantly decline.

In C99/N141I cells that produced remarkably high levels of Aβ42, total Aβ decreased gradually and the mobility of total Aβ shifted slightly upward on Tris/Tricine gels as DAPT concentrations increased (Figure 4B). On Tris/Tricine/8 M urea gels, the levels of Aβ40 and Aβ42 decreased in a dose-dependent manner but the levels of Aβ42 decreased more gradually than those of Aβ40. A striking characteristic of C99/N141I cells was the accumulation of Aβ45. The levels of Aβ45 increased gradually to a maximum at 1−2 μM and then decreased only slightly at above 2 μM. Because Aβ45 was discernible even at 20 μM (data not shown), it seemed that DAPT failed to suppress completely the cleavage at the Aβ45 site (at the carboxyl terminus of Ileu-45). The levels of Aβ46 increased slightly and gradually declined at above 1 μM. Moreover, the two bands having the same mobility as those of Aβ48 and Aβ49 were again detectable, as in C99/wtPS2. Both Aβ species decreased gradually as DAPT concentrations increased. The treatment of these cell lines with L685,458 uniformly suppressed the production of all of the Aβ species (data not shown). It should be noted that Aβ45 was not detectable in the medium of C99/N141I cells even in the presence of 1 μM DAPT, despite its intracellular accumulation (data not shown).

DISCUSSION

In the present study, we investigated alterations in the levels of intracellular longer Aβ species caused by DAPT, using various CHO cell lines coexpressing βCTF and human wt or mtPS1/2 (see Table 1 for the summary). Similar longer Aβ species were detectable within these cells as in CHO cells that coexpress APP and wt or mtPS1/2 (*21*). Overall, differential accumulations of longer Aβ, as observed in the parental C99 cells (*21*), were found in all of the C99/wt or mtPS1/2 cells examined. These longer Aβs include Aβ43, Aβ45, Aβ46, Aβ48, and presumably Aβ49. Two more nontransition-state analogue inhibitors, compound E and sulfonamide, were tested and found to cause similar accumulations of longer Aβ (parts A and B of Figure 1; see ref *20*). Thus, intracellular accumulations of longer Aβ are an important characteristic of nontransition-state analogue inhibitors. In a striking contrast, WPE-III-31C (Figure 1C) and L685,458 (*21*) suppressed uniformly the levels of all of the longer Aβs. The distinct effects of these two classes of inhibitors may reflect their distinct binding sites on the γ-secretase complex (*29*, *30*).

Table 1: Summary of DAPT Effects on the Intracellular Aβ Levels in Various Transfectants[a]

Aβ species / Cell line	Aβ40	Aβ42	Aβ43	Aβ45	Aβ46	Aβ48	Aβ49
C99/wt PS1	↘	↘	↗↘		↗↘		
C99/mtPS1 (M146L)	↘	↘	↗↘		↗↘		
C99/mtPS1 (M233T)	↘	→↘	→↘		↗↘	↗↘	
C99/mtPS1 (G384A)	↘	↘	↘		↗↘		
C99/wtPS2	↘	↘			↗↘	→	↗
C99/mtPS2 (N141I)	↘	↘		↗↘	↗↘	↘	↘

[a] →indicates no changes in the levels; ↘, decrease in the levels; ↗, increase in the levels; and ↗↘, monophasic accumulation. Blank, undetectable.

Here, the identification of the longer Aβ species relied exclusively upon the SDS/urea gel systems, as previously described (*21*). Only nontruncated Aβ species were collected by immunoprecipitation with BAN50, and subsequently, the species beginning at Asp-1 were identified by Western blotting with 82E1, N-end-specific Aβ antibody, using a Tris/Tricine/8 M urea gel. The Aβ1-X species were identified by their mobility, on the basis of the observation that they invariably comigrate with the corresponding authentic Aβs even under different gel conditions. The mass spectrometric observation validated the SDS/urea gel-based determination of Aβ43 and Aβ46 (*21*) and Aβ45.[2] However, (time-of-flight) mass spectrometry failed to identify Aβ48 and Aβ49, presumably because of their high degree of hydrophobicity. Even with the immunoprecipitate from the lysates of CHO cells coexpressing APP and M233T mtPS1, which should have relatively high levels of Aβ48, an unambiguous mass signal for Aβ48 was undetectable (*21*; see also Figure 3A). Reliability of the gel-based identification would be further strengthened by a particular relationship between the longest Aβs and AICDs. CHO cell-derived γ-secretase produced AICD50−99 and AICD49−99 at a proportion of ~7:3, while M233T mtPS1-γ-secretase released a much larger proportion of AICD49−99 (*17*). In the former case, the two longest Aβs corresponding to authentic Aβ48 and Aβ49 were detected, while in the latter case, only one Aβ corresponding to Aβ48 was detected in the CHAPSO-solubilized system by using the SDS/urea gel system II.[3] This strongly suggests that the SDS/urea gel-based identification of longer Aβs up to Aβ49 is accurate.

In C99/wtPS1 and C99/M146L mtPS1 cells, differential accumulations of Aβ43 and Aβ46 were found as observed in the parental C99 cells (Figure 2). These cell lines produced a relatively large proportion of Aβ40, and thus, this raises the possibility that marked accumulation of Aβ43 and Aβ46 is associated with a large decrease in the Aβ40 levels. However, it was not the case with C99/wtPS2 cells. In this cell line, the levels of Aβ43 and Aβ46 were significantly lower under nontreated conditions when compared with those in C99/wtPS1 cells and only Aβ46 and not Aβ43 exhibited a minimal accumulation in response to DAPT, concomitant with a large decrease in the Aβ40 levels (Figure 4A). In addition, PS2-γ-secretase appears to be more susceptible to DAPT than PS1-γ-secretase: Aβ40 was definitely detectable at 0.25 μM DAPT in C99/wtPS1 cells, whereas it was almost undetectable at the same concentration in C99/wtPS2 cells (Figures 2A and 4A). The different sensitivity of PS1- and PS2-γ-secretases to inhibitors was previously reported (*31*). Thus, it is most likely that PS1- and PS2-γ-secretases have distinct properties for cleaving the transmembrane domain of βCTF.

Among the longer Aβs, Aβ46 was the only species that accumulated commonly across all cell lines. Alterations in the levels of Aβ43 varied greatly and were not consistent among the cell lines. No accumulation of Aβ43 was noted in C99/wtPS2 cells that produce a large amount of Aβ40. Overall, a decrease in the levels of Aβ40 was followed by at least some increase in the level of Aβ46. This reciprocal change between Aβ40 and Aβ46 levels was also observed following the treatment with compound E and sulfonamide (parts A and B of Figure 1). These suggest a close relationship between Aβ40 and Aβ46 production. Consistent with this, blocking the cleavage at the midportion of γ- and ϵ-sites (ζ-cleavage site) using a Trp stretch remarkably suppressed the generation of Aβ40/42 (*32*). Thus, the cleavage at the Aβ46 site (Val-46) may be essential for Aβ40 generation, suggesting the involvement of stepwise processing.

As previously proposed, the cleavage sites associated with Aβ40 production fit well with an α-helical model of the transmembrane domain of βCTF (*21*). Val-46, Thr-43, and Val-40 are aligned on one surface of βCTF. Differential accumulations of Aβ43 and Aβ46 following treatment with DAPT are best explained by the assumption that Aβ46 is successively cleaved at every third residue by the same catalytic site and that cleavage at the Aβ40 site (Val-40) is most susceptible to DAPT, followed by cleavages at the Aβ43 (Thr-43) and Aβ46 sites (Val-46). However, this assumption cannot explain the alterations observed in compound E-treated C99 cells and DAPT-treated C99/wtPS2 cells: Aβ43 did not accumulate in these cell lines, whereas Aβ46 did accumulate. Another explanation would be that the Aβ40, Aβ43, and Aβ46 sites are cleaved almost simultaneously by two to four catalytic sites of the γ-secretase complex that have differential sensitivities to inhibitors (see ref *33*).

In the cell-free and CHAPSO-solubilized systems, only two AICDs, 49−99 and 50−99, but no longer AICD, were confirmed by mass spectrometry (*17*).[4] In addition, Aβ48 and Aβ49, potential counterparts of the two AICDs, can be processed to Aβ40/42 (*18*). Thus, it is most reasonable to postulate that the ϵ-cleaved, longest Aβs (Aβ48 and Aβ49) are the immediate substrates for produced Aβ40/42. They are stepwisely processed along the α-helical surface of βCTF at every third or sixth residue from the ϵ- (or ζ-) cleavage site to the γ-cleavage site. These cleavage sites may differ from each other in their susceptibility to inhibitors. Transi-

[2] Y. Tanimura, G. Dolios, Y. Ihara, R. Wang, and M. Morishima-Kawashima, unpublished observations.

[3] N. Kakuda and S. Yagishita, unpublished observations.

[4] N. Kakuda, S. Funamoto, and Y. Ihara, unpublished data.

tion-state analogue inhibitors may preferentially suppress the ϵ- and/or ζ-cleavage, while nontransition-state analogue inhibitors may suppress most preferentially γ-cleavage and to relatively less extents ζ- and ϵ-cleavages. Moreover, the most susceptible cleavage sites would differ even among individual nontransition-state inhibitors. For example, DAPT most preferentially suppresses the Aβ40 site, followed by the Aβ43 and Aβ46 sites, while compound E may suppress the Aβ40 and Aβ43 sites at a similar efficiency, followed by the Aβ46 site. Compared with the Aβ40 and Aβ43 sites, the Aβ46 site is most resistant to nontransition-state analogue inhibitors. This may explain why Aβ49 is usually undetectable even under inhibitor-treated conditions and why a large or small accumulation of Aβ46 is the only characteristic for all nontransition-state analogue inhibitors.

If the same α-helical model is applied to Aβ42 production, Thr-48, Ile-45, and Ala-42, which align on one surface of βCTF, would undergo stepwise cleavages producing Aβ48, Aβ45, and finally Aβ42. In the present study, three kinds of mutant PS cell lines (C99/M233T and C99/G384A mtPS1 cells and C99/N141I mtPS2 cells) were examined to test the above hypothesis. In C99/G384A cells, no accumulation of longer Aβs was detected. except for minimal accumulation of Aβ46, which may be linked to the production of Aβ40 (Figure 3B). In C99/M233T cells, DAPT caused a minimal accumulation of Aβ48, whereas the levels of Aβ42 were maintained even at higher DAPT concentrations and decreased only gradually (Figure 3A). On the other hand, in C99/N141I cells, there was a marked accumulation of Aβ45, concomitantly with a large decrease in Aβ42 levels (Figure 4B). A very small accumulation of Aβ48 was also observed. Thus, in the latter two lines, there were some relationships among Aβ42, Aβ45, and Aβ48 production, but an association between the cleavages at the Aβ42 and Aβ45 sites was obvious only in N141I mtPS2 cells. No obvious relationship between the levels of Aβ42, Aβ45, and Aβ48 in mtPS1-transfected cells may be in part related to the failure of DAPT inhibition in the production of Aβ40/42 from Aβ48 but not from Aβ49 (*18*). High resistance of the Aβ42 levels to DAPT in C99/M233T and C99/G384A cells may be explained by this observation. Overall, there is no definite evidence for stepwise processing for Aβ42 production in mtPS1 cells. These may suggest that Aβ42-producing machinery is not under strict regulation as found in Aβ40-producing machinery and would be susceptible to a greater extent to many kinds of perturbation (*34*, *35*).

In summary, the complicated patterns of accumulation of longer Aβs can be explained on the basis of an α-helical model for unidirectional stepwise processing and γ-cleavage-predominant suppression by DAPT. The production of Aβ40 by PS1-γ-secretase is best explained in this way, but the production of Aβ42 is not necessarily consistent with the model.

ACKNOWLEDGMENT

We thank Dr. T. Iwatsubo for anti-presenilin antibodies, Dr. A. Asami for BAN50, and Dr. S. Funamoto for technical assistance with the construction of cDNAs.

SUPPORTING INFORMATION AVAILABLE

Western blots showing the expression levels of PS1 or PS2 in each C99/PS cell lines. This material is available free of charge via the Internet at http://pubs.acs.org.

REFERENCES

1. Selkoe, D. J. (2001) Alzheimer's Disease: Genes, Proteins, and Therapy, *Physiol. Rev. 81*, 741−766.
2. Vassar, R., Bennett, B. D., Babu-Khan, S., Kahn, S., Mendiaz, E. A., Denis, P., Teplow, D. B., Ross, S., Amarante, P., Loeloff, R., Luo, Y., Fisher, S., Fuller, J., Edenson, S., Lile, J., Jarosinski, M. A., Biere, A. L., Curran, E., Burgess, T., Louis, J. C., Collins, F., Treanor, J., Rogers, G., and Citron, M. (1999) β-Secretase Cleavage of Alzheimer's Amyloid Precursor Protein by the Transmembrane Aspartic Protease BACE, *Science 286*, 735−741.
3. Iwatsubo, T., Odaka, A., Suzuki, N., Mizusawa, H., Nukina, N., and Ihara, Y. (1994) Visualization of Aβ42(43) and Aβ40 in Senile Plaques with End-Specific Aβ Monoclonals: Evidence That an Initially Deposited Species Is Aβ42(43), *Neuron 13*, 45−53.
4. McGowan, E., Pickford, F., Kim, J., Onstead, L., Eriksen, J., Yu, C., Skipper, L., Murphy, M. P., Beard, J., Das, P., Jansen, K., DeLucia, M., Lin, W. L., Dolios, G., Wang, R., Eckman, C. B., Dickson, D. W., Hutton, M., Hardy, J., and Golde, T. (2005) Aβ42 Is Essential for Parenchymal and Vascular Amyloid Deposition in Mice, *Neuron 47*, 191−199.
5. Wolfe, M. S., and Haass, C. (2000) The Role of Presenilins in γ-Secretase Activity, *J. Biol. Chem. 276*, 5413−5416.
6. Wolfe, M. S., Xia, W., Ostaszewski, B. L., Diehl, T. S., Kimberly, W. T., and Selkoe, D. J. (1999) Two Transmembran Aspartates in Presenilin-1 Required for Presenilin Endoproteolysis an γ-Secretase Activity, *Nature 398*, 513−517.
7. Steiner, H., Duff, K., Capell, A., Romig, H., Grim, M. G., Lincoln, S., Hardy, J., Yu, X., Picciano, M., Fechteler, K., Citron, M., Kopan, R., Pesold, B., Keck, S., Baader, M., Tomita, T., Iwatsubo, T., Baumeister, R., and Haass, C. (1999) A Loss of Function Mutation of Presenilin-2 Interferes with Amyloid β-Peptide Production and Notch Signaling, *J. Biol. Chem. 274*, 28669−28673.
8. Weihofen, A., Binns, K., Lemberg, M. K., Ashman, K., and Martoglio, B. (2002) Identification of Signal Peptide Peptidase, a Presenilin-Type Aspartic Protease, *Science 296*, 2215−2218.
9. Haass, C. (2004) Take Five-BACE and the γ-Secretase Quartet Conduct Alzheimer's Amyloid β-Peptide Generation, *EMBO J. 23*, 483−488.
10. Kimberly, W. T., LaVoie, M. J., Ostaszewski, B. L., Ye, W., Wolfe, M. S., and Selkoe, D. J. (2003) γ-Secretase Is a Membrane Protein Complex Comprised of Presenilin, Nicastrin, Aph-1, and Pen-2, *Proc. Natl. Acad. Sci. U.S.A. 100*, 6382−6387.
11. Takasugi, N., Tomita, T., Hayashi, I., Tsuruoka, M., Niimura, M., Takahashi, Y., Thinakaran, G., and Iwatsubo, T. (2003) The Role of Presenilin Cofactors in the γ-Secretase Complex, *Nature 422*, 438−441.
12. Edbauer, D., Winkler, E., Regula, J. T., Pesold, B., Steiner, H., and Haass, C. (2003) Reconstitution of γ-Secretase Activity, *Nat. Cell Biol. 5*, 486-488.
13. Gu, Y., Misonou, H., Sato, T., Dohmae, N., Takio, K., and Ihara, Y. (2001) Distinct Intramembrane Cleavage of the β-Amyloid Precursor Protein Family Resembling γ-Secretase-like Cleavage of Notch, *J. Biol. Chem. 276*, 35235−35238.
14. Sastre, M., Steiner, H., Fuchs, K., Capell, A., Multhaup, G., Condron, M. M., Teplow, D. B., and Haass, C. (2001) Presenilin-Dependent γ-Secretase Processing of β-Amyloid Precursor Protein at a Site Corresponding to the S3 Cleavage of Notch, *EMBO Rep. 2*, 835−841.
15. Yu, C., Kim, S. H., Ikeuchi, T., Xu, H., Gasparini, L., Wang, R., and Sisodia, S. S. (2001) Characterization of a Presenilin-Mediated Amyloid Precursor Protein Carboxyl-Terminal Fragment γ, *J. Biol. Chem. 276*, 43756−43760.
16. Weidemann, A., Eggert, S., Reinhard, F. B. M., Vogel, M., Paliga, K., Baier, G., Masters, C. L., Beyreuther, K., and Evin, G. (2002) A Novel ϵ-Cleavage within the Transmembrane Domain of the Alzheimer Amyloid Precursor Protein Demonstrates Homology with Notch Processing, *Biochemistry 41*, 2825−2835.
17. Sato, T., Dohmae, N., Qi, Y., Kakuda, N., Misonou, H., Mitsumori, R., Maruyama, H., Koo, E. H., Haass, C., Takio, K., Morishima-Kawashima, M., Ishiura, S., and Ihara, Y. (2003) Potential Link

between Amyloid β-Protein 42 and C-terminal Fragment γ49−99 of β-Amyloid Precursor Protein, *J. Biol. Chem. 278*, 24294−24301.
18. Funamoto, S., Morishima-Kawashima, M., Tanimura, Y., Hirotani, N., Saido, T. C., and Ihara, Y. (2004) Truncated Carboxyl-Terminal Fragments of β-Amyloid Precursor Protein Are Processed to Amyloid β-Proteins 40 and 42, *Biochemistry 43*, 13532−13540.
19. Zhao, G., Cui, M. Z., Mao, G., Dong, Y., Tan, J., Sun, L., and Xu, X. (2005) γ-Cleavage Is Dependent on ζ-Cleavage During the Proteolytic Processing of Amyloid Precursor Protein within Its Transmembrane Domain, *J. Biol. Chem. 280*, 37689−37697.
20. Zhao, G., Mao, G., Tan, J., Dong, Y., Cui, M. Z., Kim, S. H., and Xu, X. (2004) Identification of a New Presenilin-Dependent ζ-Cleavage Site within the Transmembrane Domain of Amyloid Precursor Protein, *J. Biol. Chem. 279*, 50647−50650.
21. Qi-Takahara, Y., Morishima-Kawashima, M., Tanimura, Y., Dolios, G., Hirotani, N., Horikoshi, Y., Kametani, F., Maeda, M., Saido, T. C., Wang, R., and Ihara, Y. (2005) Longer Forms of Amyloid β-Protein: Implications for the Mechanism of Intramembrane Cleavage by γ-Secretase, *J. Neurosci. 25*, 436−445.
22. Suzuki, N., Cheung, T. T., Cai, X. D., Okada, A., Otvos, L., Jr., Eckman, C., Golde, T. E., and Younkin, S. G. (1994) An Increased Percentage of Long Amyloid β Protein Secreted by Familial Amyloid β Protein Precursor (βAPP717) Mutants, *Science 264*, 1336−1340.
23. Qi, Y., Morishima-Kawashima, M., Sato, T., Mitsumori, R., and Ihara, Y. (2003) Distinct Mechanisms by Mutant Presenilin 1 and 2 Leading to Increased Intracellular Levels of Amyloid β-Protein 42 in Chinese Hamster Ovary Cells, *Biochemistry 42*, 1042−1052.
24. Shearman, M. S., Beher, D., Clarke, E. E., Lewis, H. D., Harrison, T., Hunt, P., Nadin, A., Smith, A. L., Stevenson, G., and Castro, J. L. (2000) L-685,458, an Aspartyl Protease Transition State Mimic, Is a Potent Inhibitor of Amyloid β-Protein Precursor γ-Secretase Activity, *Biochemistry 39*, 8698−8704.
25. Dovey, H. F., John, V., Anderson, J. P., Chen, L. Z., de Saint Andrieu, P., Fang, L. Y., Freedman, S. B., Folmer, B., Goldbach, E., Holsztynska, E. J., Hu, K. L., Johnson-Wood, K. L., Kennedy, S. L., Kholodenko, D., Knops, J. E., Latimer, L. H., Lee, M., Liao, Z., Lieberburg, I. M., Motter, R. N., Mutter, L. C., Nietz, J., Quinn, K. P., Sacchi, K. L., Seubert, P. A., Shopp, G. M., Thorsett, E. D., Tung, J. S., Wu, J., Yang, S., Yin, C. T., Schenk, D. B., May, P. C., Altstiel, L. D., Bender, M. H., Boggs, L. N., Britton, T. C., Clemens, J. C., Czilli, D. L., Dieckman-McGinty, D. K., Droste, J. J., Fuson, K. S., Gitter, B. D., Hyslop, P. A., Johnstone, E. M., Li, W. Y., Little, S. P., Mabry, T. E., Miller, F. D., Ni, B., Nissen, J. S., Porter, W. J., Potts, B. D., Reel, J. K., Stephenson, D., Su, Y., Shipley, L. A., Whitesitt, C. A., Yin, T., and Audia, J. E. (2001) Functional γ-Secretase Inhibitors Reduce β-Amyloid Peptide Levels in Brain, *J. Neurochem. 76*, 173−181.
26. Seiffert, D., Bradley, J. D., Rominger, C. M., Rominger, D. H., Yang, F., Meredith J. E., Jr., Wang, Q., Roach, A. H., Thompson, L. A., Spitz, S. M., Higaki, J. N., Prakash, S. R., Combs, A. P., Copeland, R. A., Arneric, S. P., Hartig, P. R., Robertson, D. W., Cordell, B., Stern, A. M., Olson, R. E., and Zaczek, R. (2000) Presenilin-1 and -2 Are Molecular Targets for γ-Secretase Inhibitors, *J. Biol. Chem. 275*, 34086−34091,
27. Rishton, G. M., Retz, D. M., Tempest, P. A., Novotny, J., Kahn, S., Treanor, J. J. S., Lile, J. D., and Citron, M. (2000) Fenchylamine Sulfonamide Inhibitors of Amyloid β Peptide Production by the γ-Secretase Proteolytic Pathway: Potential Small-Molecule Therapeutic Agents for the Treatment of Alzheimer's Disease, *J. Med. Chem. 43*, 2297−2299.
28. Esler, W. P., Kimberly, W. T., Ostaszewski, B. L., Ye, W., Diehl, T. S., Selkoe, D. J., and Wolfe M. S. (2002) Activity-Dependent Isolation of the Presenilin-γ-secretase Complex Reveals Nicastrin and a γ Substrate, *Proc. Natl, Acad. Sci. U.S.A. 99*, 2720−2725.
29. Tian, G., Ghanekar, S. V., Aharony, D., Shenvi, A. B., Jacobs, R. T., Liu, X., and Greenberg, B. D. (2003) The Mechanism of γ-Secretase: Multiple Inhibitor Binging Sites for Transition State Analogs and Small Molecule Inhibitors, *J. Biol. Chem. 278*, 28968−28975.
30. Kornilova, A. Y., Das, C., and Wolfe, M. S. (2003) Differential Effect of Inhibitors on the γ-Secretase Complex, *J. Biol. Chem. 278*, 16470−16473.
31. Lai, M. T., Chen, E., Crouthamel, M. C., DiMuzio-Mower, J., Xu, M., Huang, Q., Price, E., Register, R. B., Shi, X. P., Donoviel, D. B., Bernstein, A., Hazuda, D., Gardell, S. T., and Li, Y. M. (2003) Presenilin-1 and Presenilin-2 Exhibit Distinct yet Overlapping γ-Secretase Activities, *J. Biol. Chem. 278*, 22475−22481.
32. Sato, T., Tanimura, Y., Hirotani, N., Saido, T. C., Morishima-Kawashima, M., and Ihara, Y. (2005) Blocking the Cleavage at Midportion between γ- and ϵ-Sites Remarkably Suppresses the Generation of Amyloid β-Protein, *FEBS Lett. 579*, 2907−2912.
33. Schroeter, E. H., Ilagan, M. X., Brunkan, A. L., Hecimovic, S., Li, Y. M., Xu, M., Lewis, H. D., Saxena, M. T., De Strooper, B., Coonrod, A., Tomita, T., Iwatsubo, T., Moore, C. L., Goate, A., Wolfe, M. S., Shearman, M., and Kopan, R. (2003) A Presenilin Dimer at the Core of the γ-Secretase Enzyme: Insights from Parallel Analysis of Notch 1 and APP Proteolysis, *Proc. Natl. Acad. Sci. U.S.A. 100*, 13075−13080.
34. Eriksen, J. L., Sagi, S. A., Smith, T. E., Weggen, S., Das, P., McLendon, D. C., Ozols, V. V., Jessing, K. W., Zavitz, K. H., Koo, E. H., and Golde, T. E. (2003) NSAIDs and Enantiomers of Flurbiprofen Target γ-Secretase and Lower Aβ42 *in Vivo*, *J. Clin. Invest. 112*, 440−449.
35. Kukar, T., Murphy, M. P., Eriksen, J. L., Sagi, S. A., Weggen, S., Smith, T. E., Ladd, T., Khan, M. A., Kache, R., Beard, J., Dodson, M., Merit, S., Ozols, V. V., Anastasiadis, P. Z., Das, P., Fauq, A., Koo, E. H., and Golde, T. E. (2005) Diverse Compounds Mimic Alzheimer Disease-Causing Mutations by Augmenting Aβ42 Production, *Nat. Med. 11*, 545−550.

BI0521846